Available online at www.sciencedirect.com
ScienceDirect
Biochemical and Biophysical Research Communications 361 (2007) 256–262
BBRC
www.elsevier.com/locate/ybbrc

The conserved glycine/alanine residue of the active-site loop containing the putative acetylCoA-binding motif is essential for the overall structural integrity of *Mesorhizobium loti* arylamine *N*-acetyltransferase 1

Noureddine Atmane [a,1], Julien Dairou [a,b,1], Delphine Flatters [c], Marta Martins [a], Benjamin Pluvinage [a], Philippe Derreumaux [b,d], Jean-Marie Dupret [a,b], Fernando Rodrigues-Lima [a,b,*]

[a] *Laboratoire de Cytophysiologie et Toxicologie Cellulaire (EA 1553), Université Paris Diderot—Paris 7, 75005 Paris, France*
[b] *UFR de Biochimie, Université Paris Diderot—Paris 7, 75005 Paris, France*
[c] *Equipe de Bioinformatique Génomique et Moléculaire, INSERM UMR-S 726, Université Paris Diderot—Paris 7, 75005 Paris, France*
[d] *Laboratoire de Biochimie Théorique, UPR 9080 CNRS, Institut de Biologie Physico-Chimique, Universite Paris Diderot—Paris 7, 75005 Paris, France*

Received 9 July 2007
Available online 17 July 2007

Abstract

The arylamine *N*-acetyltransferases are important xenobiotic-metabolizing enzymes that catalyze an acetyl group transfer from acetylCoA to arylamine substrates. NAT enzymes possess an active-site loop (the active-site P-loop) involved in substrate binding and selectivity. The Gly/Ala residue present at the start of the active-site P-loop, although conserved in all NAT enzymes, is not involved in the catalytic mechanism or substrate binding. Here we show that a small amino acid (such as Gly or Ala) at this position is important not only for maintaining the functions of the active-site P-loop but, more surprisingly, also important for maintening the overall structural integrity of NAT enzymes. Our data thus suggest that in addition to its role in substrate binding and selectivity, the active-site P-loop could play a wider structural role in NAT enzymes.

Keywords: Arylamine *N*-acetyltransferase; P-loop; Active-site; Steric hindrance; Site-directed mutagenesis

Arylamine *N*-acetyltransferases (NAT) are xenobiotic-metabolizing enzymes (XME) catalyzing the transfer of an acetyl group from acetylCoA (AcCoA) to the nitrogen or oxygen atom of arylamines, hydrazines, and their *N*-hydroxylated metabolites [1]. These XME have a key role in the detoxification and metabolic activation of numerous xenobiotics, including therapeutic drugs and carcinogens.

NAT enzymes have been identified and characterized in eukaryotic and prokaryotic species [2]. It has been suggested that a structural P-loop motif present in all NAT enzymes is involved in AcCoA binding [2]. Moreover, the Gly126 residue of the putative P-loop of *Salmonella typhimurium* NAT was shown to contribute to AcCoA binding [3]. NAT P-loop motif is part of a 10- to 12-amino acid loop (referred as the active-site P-loop) involved in formation of the active site pocket of NAT enzymes [3]. The active-site P-loop is a structurally conserved active-site region (RMSD < 1.5 Å) [6,7] involved in the substrate binding and selectivity of NAT enzymes [3–5]. The release of the structure of human NAT2 in complex with CoA will provide important clue on the residues in AcCoA binding.

A highly conserved Gly residue (Gly129 in MlNAT1) is located at the start of the active-site P-loop in NAT enzymes

Abbreviations: NAT, arylamine *N*-acetyltransferase; RMSD, root mean square deviation; RMSF, root mean square fluctuation; MLNAT1, *Mesorhizobium loti* NAT1.

* Corresponding author. Address: Laboratoire de Cytophysiologie et Toxicologie Cellulaire (EA 1553), Université Paris Diderot—Paris 7, 75005 Paris, France.
E-mail address: rlima@ext.jussieu.fr (F. Rodrigues-Lima).

[1] These authors contributed equally to this work.

0006-291X/$ - see front matter © 2007 Elsevier Inc. All rights reserved.
doi:10.1016/j.bbrc.2007.07.034

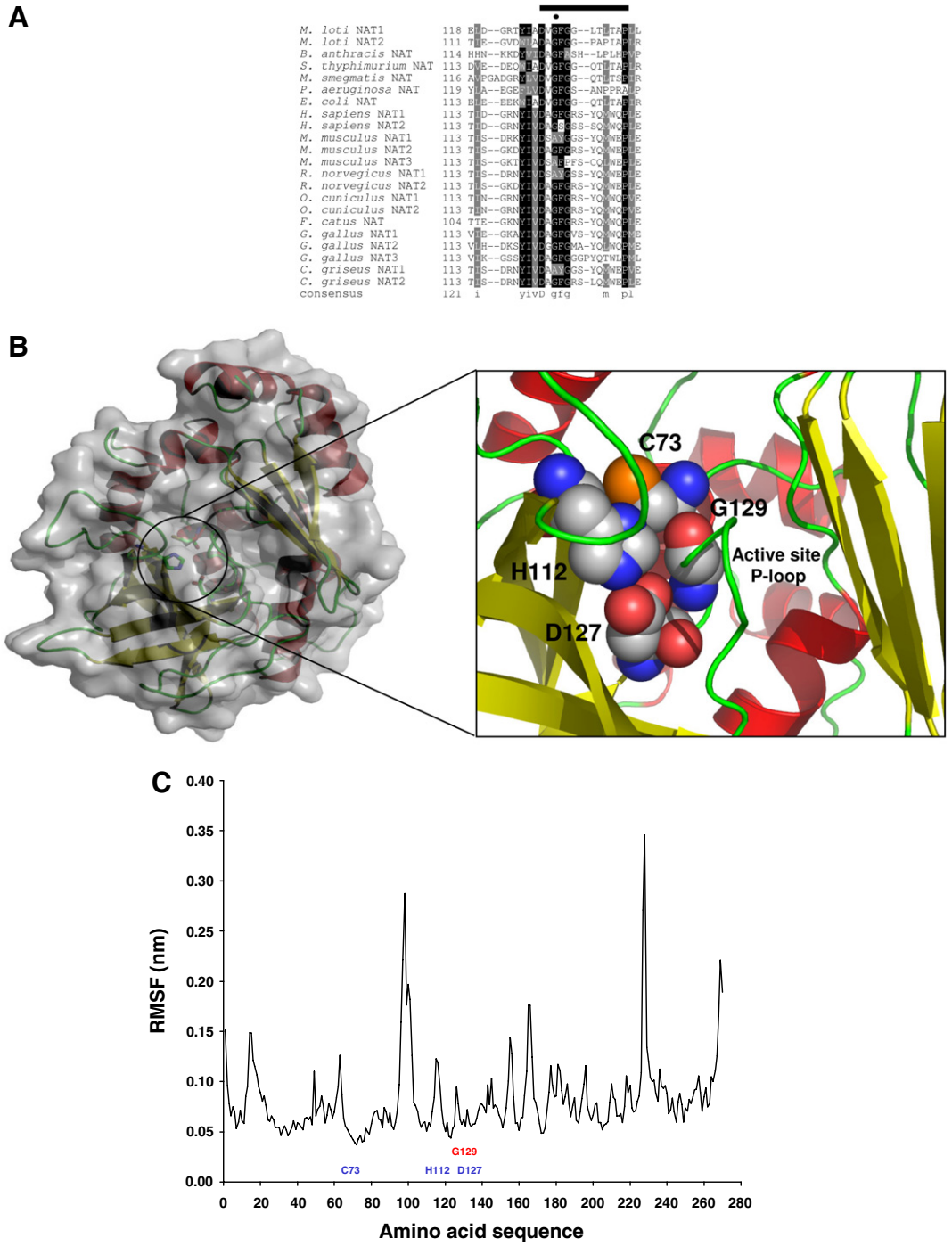

Fig. 1. Conservation of the active-site P-loop Gly/Ala residue in NAT enzymes. (A) Multiple sequence alignment showing the active-site P-loops of various eukaryotic and prokaryotic NAT enzymes. The first line of the alignment corresponds to the MlNAT1 enzyme used in this study. Amino-acid sequences were aligned using Clustal W1.8. The active-site P-loop of MlNAT1 is indicated by the black bar. The conserved Gly/Ala position is shown by a dot. (B) Representation of the crystal structure of MlNAT1. The catalytic triad residues (Cys73, His112, and Asp127) and the active-site P-loop Gly residue (Gly129) are presented as space-filling atoms (van der Waals volumes). (C) Root mean square fluctuation (RMSF) analysis of the Cα atoms of MlNAT1 by MD. Variations of the spatial position of each Cα over the dynamics simulation (RMSF) are in nanometers (nm). The catalytic triad residues are indicated by a blue dot. The Gly129 residue is indicated by a red dot. (For interpretation of the references to colour in this figure legend, the reader is referred to the web version of this article.)

(Fig. 1A) [3]. In a limited number of NAT enzymes (such as a mouse isoform), an alanine replaces the Gly residue (Fig. 1), with no obvious effects on activity [8]. Although this Gly or Ala (Gly/Ala) residue is part of the active-site P-loop of NAT enzymes, it is not involved in the catalytic process or substrate binding [3,9,10]. We therefore investigated whether this strictly conserved Gly/Ala residue could have a more structural role in the NAT enzyme family.

Using the well characterized *Mesorhizobium loti* NAT1 isoform as model of NAT [11], we show that the presence of an amino acid with a small side chain (i.e. Gly/Ala residues) is required in this position to maintain the functions of the active-site P-loop, but also to maintain the overall structural integrity of NAT enzymes. Our results suggest that steric hindrance at this position would lead to major changes in the specific packing (van der Waals contacts) of active-site residues, leading to disruption of the overall structure of the enzyme. Therefore our data suggest that in addition to its role in substrate binding and selectivity, the active-site P-loop could play a wider structural role in NAT enzymes.

Materials and methods

Site-directed mutagenesis. The pET28Ta-MlNAT1 vector encodes the enzyme as a polyhistidine (6×His)-tagged fusion protein. Six mutant proteins in which the Gly129 residue was replaced by an Ala, Ser, Thr, Val, Ile or Pro residue were constructed with the following mutagenic primers (sense and antisense): G129A: 5′-CCGATGTCGCGTTCGGCGG-3′, 5′-CCGCCGAACGCGACATCGG-3′; G129S: 5′-CCGATGTCAGTTTCGGCGG-3′, 5′-CCGCCGAAACTGACATCGG-3′; G129T: 5′-CCGATGTCACGTTCGGCGG-3′, 5′-CCGCCGAACGTGACATCGG-3′; G129V: 5′-CCGATGTCGTGTTCGGCGG-3′, 5′-CCGCCGAACACGACATCGG-3′; G129I: 5′-CCGATGTCATTTTCGGCGG-3′, 5′-CCGCCGAAAATGACATCGG-3′; G129P: 5′-CCGATGTCCCGTTCGGCGG-3′, 5′-CCGCCGAACGGGACATCGG-3′ . The N- and C-terminal primers used were: 5′-AAGGATCCATGAACGATGCTCCTCCC-3′ and 5′-AACTCGAGTCATGCGTTGGTCTCCAC.

Protein production and purification. Bacteria were induced (5 h at 37 °C) with 0.5 mM isopropyl-1-thio-β-D-galactopyranoside (IPTG). After centrifugation, the pellet was incubated (1 h at 4 °C) in 20 ml of PBS with lysozyme, protease inhibitors and Triton X-100 (0.1%). Following sonication and centrifugation, the insoluble fraction was washed with PBS. The supernatant was incubated with Ni^{2+}–agarose (2 h, 4 °C) and the MlNAT1 proteins eluted with 300 mM imidazole. Purified enzymes were reduced with DTT and dialyzed against 25 mM Tris–HCl, pH 7.5, 1 mM EDTA.

Enzyme assay. The activity of the recombinant enzymes was assayed by measuring the rate of hydrolysis of acetylCoA (first substrate) in the presence of PAS (arylamine substrate), using 5,5′-dithio-bis-2-nitrobenzoic acid (DTNB), as previously described [12]. Data are expressed as means ± SD. Apparent kinetic parameters (Vm_{app} and Km_{app}) were determined by non linear regression from Michaelis–Menten plots. For bi–bi ping–pong mechanisms (as for NAT), apparent Vm/apparent Km ratios are equal to true kinetic parameter ratios (Vm/Km) [13]. Vm_{app}/Km_{app} ratios were therefore used for the comparison of catalytic efficiencies.

SDS–PAGE and Western blotting. Protein concentrations were determined using the Bradford assay (Bio-Rad). A polyclonal anti-*S. typhimurium* NAT antibody (provided by Prof. Sim, Oxford) or a monoclonal anti-6×His tag antibody were used in Western-blots. The fraction of protein in the samples that is MlNAT1 was estimated from SDS–PAGE gels and Western-blots by densitometry using the MultiGauge program (FujiFilm). Factors deduced from these analyses were used to correct specific activities.

Computational analysis of intrinsic protein stability and first-order heat inactivation rate constants determination. The stability of the MlNAT1 and mutant proteins was estimated in silico by calculating folding free energies ($\Delta G_{folding}$, kcal/mol) using the FOLD-X force field [14]. FOLD-X calculations of the mutants were carried out using the wild-type MlNAT1 structure. Moreover, the intrinsic stability of the recombinant MlNAT1 and mutant enzymes was also determined by measuring first-order heat inactivation constants (k_{inact}) at 50 °C as previously described [15].

Molecular dynamics (MD) simulations were carried out with the MlNAT1 cristal structure and with Gly129 mutant MlNAT1 models generated with the Modeller as previously described [16].

Results

Purification and activity of recombinant MlNAT1 proteins

MD simulations indicated that the Cα atoms of MlNAT1 deviates by 2 Å rms from the minimized positions within 4 ns. Analysis of the RMSF showed that Gly129 (Fig. 1C) and the catalytic triad amino acids display little flexibility (RMSF ≈ 0.5–0.6 Å). Identical results were obtained for the other known NAT structures (*S. typhimurium*, *Mycobacterium smegmatis*, *Pseudomonas aeruginosa* and *Homo sapiens* NATs) using MD simulations spanning 20 ns time-scale (not shown). While the reduced flexibility of catalytic residues is expected since they are under conformational constraints [6,7], the low flexibility of the MlNAT1 Gly129 residue (and its equivalent Gly residue in other NAT structures) is consistent with its potential structural role. We therefore replaced the Gly129 residue of MlNAT1 with polar/apolar residues differing in bulkiness (Ala, Ser, Thr, Val, Ile, and Pro) and conformational rigidity. No differences in the growth and numbers of *Escherichia coli* cells were observed, indicating that no mutant was deleterious for the bacterium. The G129A, G129S and WT MlNAT1 cultures (1 l) yielded ~30 mg of protein after Ni^{2+}–agarose purification, whereas the other mutants yielded 0.75–0.5 mg of protein. SDS–PAGE (Fig. 2A) showed that the G129A and G129S mutants gave levels of pure soluble protein similar to those of WT MlNAT1. Conversely, the G129T, G129V, G129I and G129P mutants produced only small amounts of NAT proteins (G129T and G129V protein levels being higher than those of G129I and G129P) and contained contaminants. Densitometry analysis indicated that the amounts of G129T and G129V mutant proteins were only about one fifth those of the G129A, G129S, and WT MlNAT1 proteins. G129I and G129P were produced in even smaller amounts (lower by a factor of 10; not shown). Similar amounts of G129A, G129S, and WT MlNAT1 proteins were purified (Fig. 2A). Identical results were obtained in western-blots with an anti-histidine antibody (not shown). Attempts to further purify the G129T, G129V, G129I,, and G129P mutants were unsuccessful.

We investigated whether the low levels of production of the G129T, G129V, G129I, and G129P mutants were due to the formation of insoluble protein aggregates (inclusion bodies). Western-blots (Fig. 2B and C) showed that the mutant and WT enzymes were mostly present in the soluble fraction (Fig. 2B). As observed with the Ni^{2+}–agarose-purified proteins (Fig. 2A), the G129A and G129S mutants and WT MlNAT1 were produced in much larger amounts than the other mutants. Conversely, small amounts (about one sixth those in the soluble fraction) of the G129A, G129S, and G129T mutants and the WT MlNAT1 protein

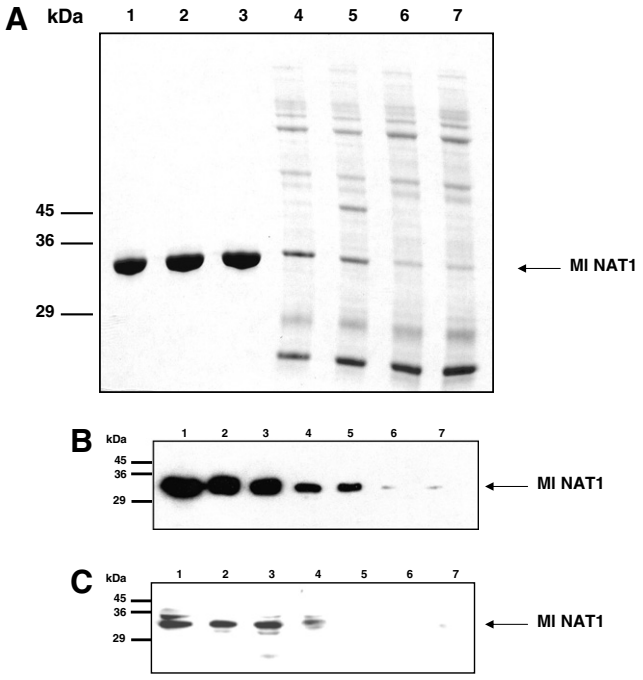

Fig. 2. SDS–PAGE analysis of recombinant WT MlNAT1 and Gly129 mutants A. Purified proteins (2 μg) were separated by SDS–PAGE under reducing conditions and stained with Coomassie blue (WT MlNAT1: lane 1; G129A: lane 2, G129S: lane 3, G129T: lane 4, G129V: lane 5, G129I: lane 6, G129P: lane 7). (B) The soluble fraction of *E. coli* lysates was subjected to SDS–PAGE under reducing conditions (1 μg protein) and western blotting with a polyclonal antibody against the *Salmonella typhimurium* NAT (WT MlNAT1: lane 1, G129A: lane 2, G129S: lane 3, G129T: lane 4, G129V: lane 5, G129I: lane 6, G129P: lane 7). C. The insoluble fraction of the *E. coli* lysates was also analyzed (1 μg protein) as in (A).

were detected in the insoluble fraction, and the G129V, G129I, and G129P mutants were undetectable in this fraction (Fig. 2C). Thus, the small amounts of soluble protein obtained with the G129T, G129V, G129I, and G129P mutants were not due to accumulation in inclusion bodies and resulted instead from degradation within the bacteria [17]. Protein yield and solubility were not dependent on temperature and IPTG concentration (data not shown).

Specific activities of the Ni^{2+}–agarose-purified proteins (corrected for the amount of MlNAT1 protein in the samples) were determined under the same conditions for each mutant (Table 1). The G129A mutant and the WT protein had similar specific activities. The G129S mutant had a slightly lower specific activity (82% that of WT enzyme). In contrast, the G129T and G129V mutants had extremely low levels of NAT activity, corresponding to less than 1% (i.e. 0.67% for G129T and 0.43% for G129V) of the specific activity for the WT enzyme.

Steady-state kinetics and conformational integrity of recombinant proteins

We carried out a steady-state kinetics analysis of the G129A and G129S mutants and the WT MlNAT1 enzyme. The low levels of activity obtained with the G129T and G129V mutants (Table 1) were not compatible with the accurate measurement of kinetic parameters, and these two mutants were therefore not included in the analysis. The G129A and WT MlNAT1 enzymes were found to display similar kinetic parameters (Vm_{app}, Km_{app}) and hence similar catalytic efficiencies (Vm_{app}/Km_{app}) (Fig. 3). Conversely, the kinetic parameters of the G129S mutant were affected. The Km_{app} value of the G129S mutant was around 2 times higher than those obtained with the WT and G129A enzymes. The Vm_{app} value of the G129S mutant was lower than that of the WT and G129A enzymes by a factor of only 1.2. The catalytic efficiency (Vm_{app}/Km_{app}) of the G129S mutant was thus 2.6 times lower than the catalytic efficiency obtained with the WT and the G129A enzyme. Similar data were obtained when another NAT substrate (2-AF) was used (data not shown). In addition, 4 ns MD simulations of the Gly129 mutants indicated that substitution of the Gly129 residue increased the conformational flexibility/mobility (1 Å RMSF variation) of the active-site P-loop amino acids (data not shown). These results may account for the effects of G129A and G129S mutations on substrate binding affinity, as some of the amino acids of the active-site P-loop are involved in substrate binding [3].

We assessed the intrinsic stability of the G129S, G129A, and WT MlNAT1 enzymes, using the method of Fretland et al. [15], which is used to assess the stability of NAT

Table 1
NAT specific activity and FOLD-X analysis of the WT MlNAT1 and Gly129 mutants

Enzyme	Volume of amino acid 129 (Å^3)	NAT activity[a] (nmol/min/mg)	Relative percentage of specific activity	ΔG folding (kcal/mol)	$\Delta\Delta G$ folding (kcal/mol)
WT	48	5078 ± 246	100	−69.52	[b]
G129A	67	4758 ± 224	94	−68.57	0.95
G129S	73	4152 ± 147[c]	82	−68.48	1.04
G129T	93	34 ± 11[c]	0.67	−64.01	5.54
G129V	105	22 ± 4[c]	0.43	−61.06	8.46
G129I	113	[b]	[b]	−50.53	18.99
G129P	97	[b]	[b]	−58.47	11.05

[a] Specific activities were corrected for the amount of MlNAT1 in the Ni^{2+}–agarose-purified samples.
[b] Very low NAT activity, which could not be measured accurately.
[c] $p < 0.05$ *versus* WT or G129A enzymes.

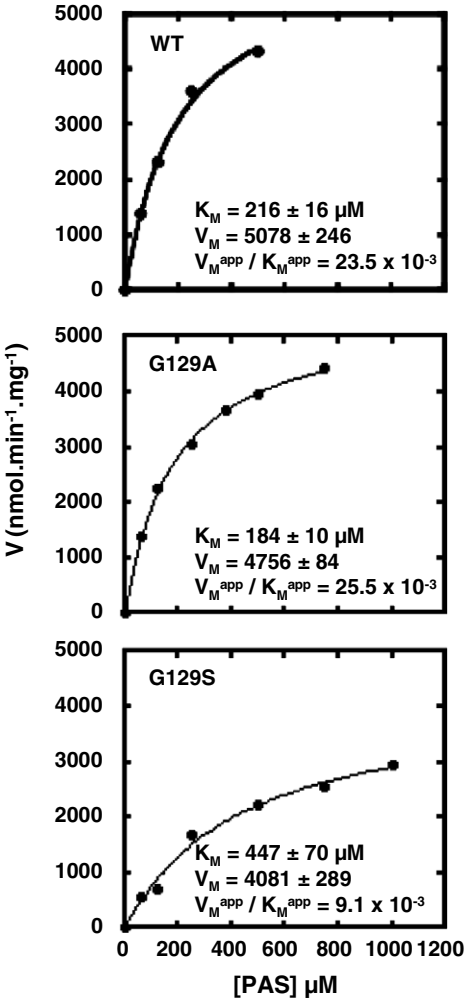

Fig. 3. Kinetic analysis of WT MlNAT1 and G129A and G129S mutant enzymes. NAT activity was measured for purified WT MlNAT1 and the G129A and G129S enzymes, using two characteristic NAT acceptor substrates: PAS and 2-AF. Data are the means of triplicate determinations. The Michaelis–Menten parameters V_M^{app} and K_m^{app} were determined by direct Michaelis–Menten equation curve fitting. V_i is plotted on the x-axis, in units of nmol/min/mg protein. V_{max}^{app} values are given in the same units and K_M^{app} values are given in units of µM.

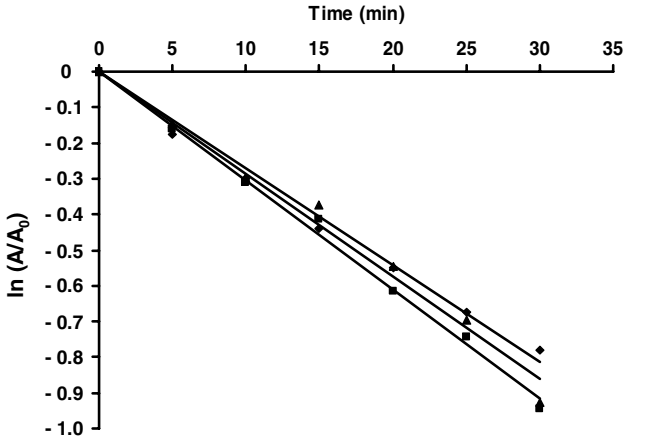

Fig. 4. Determination of first-order heat inactivation constants (k_{inact}) for WT MlNAT1 and the G129A and G129S mutants. The method of Fretland et al. [15] was used to determine k_{inact} constants. The values of k_{inact} were 0.0272 min^{-1} for WT MlNAT1 (black squares), 0.0284 min^{-1} for G129A (black triangles), and 0.0308 min^{-1} for G129S (black rhombi). (A) Residual activity at time t, A_0: enzyme activity at start.

enzymes and in particular to measure the effect of polymorphisms on NAT protein stability through determination of heat inactivation rate constants (k_{inact}) (Fig. 4). The WT MlNAT1 and G129A mutant had very similar k_{inact} values (272×10^{-4} min^{-1} for WT MlNAT1 and 280×10^{-4} min^{-1} for the G129A mutant). Conversely, the G129S mutant was slightly less stable with a k_{inact} value of 308×10^{-4} min^{-1} ($t_{1/2}$ values of 22.5 min for G129S and 25.5 min for WT MlNAT1), which might contribute to its lower catalytic efficiency [15]. We also assessed the intrinsic stability of the weakly active G129T and G129V mutant proteins. However, these proteins were too unstable for accurate k_{inact} determination. Comparisons of the fluorescence spectra of the WT enzyme and the G129A and G129S mutants revealed no detectable gross change in the conformation of these proteins (not shown).

We calculated the folding free energies ($\Delta G_{folding}$) and differences in folding free energies ($\Delta\Delta G_{folding}$) between WT and mutant enzymes, using the FOLD-X force field. This *in silico* approach has been found to yield accurate predictions [14]. Ala and Ser substitutions had modest effects on folding energy ($\Delta\Delta G_{folding} \sim 1$ kcal/mol), whereas the replacement of the Gly129 residue by amino acids larger than Ser—Thr, Val, Ile, and Pro (which has also high conformational rigidity)—led to large increases in $\Delta\Delta G_{folding}$, ranging from 5.5 kcal/mol for G129T to 19 kcal/mol for G129I (Table 1). Further analysis of the various FOLD-X components indicated that the increase in $\Delta G_{folding}$ values of these mutants resulted mostly from the van der Waals interactions (data not shown) and correlated with the bulkiness of the amino acid in position 129. These theoretical results are consistent with the location of Gly129 in the tightly packed region of the enzyme (Fig. 1A and B and [7]). The higher $\Delta G_{folding}$ values of the G129T, G129V, G129I, and G129P mutants with respect to the WT enzyme strongly suggest that these mutants are unstable and misfolded. This conclusion is fully supported by our protein production data in *E. coli* showing that these mutants did not adopt the correct conformation and were likely degraded in the bacteria [17].

Discussion

Analysis of the recombinant MlNAT1 proteins in *E.coli* indicated that replacement of the Gly129 residue by an amino acid with a van der Waals volume greater than that of Ser (73 $Å^3$), such as G129T (93 $Å^3$), G129V (105 $Å^3$), G129I (113 $Å^3$) and G129P (97 $Å^3$ also displaying extreme conformational rigidity) resulted in a large decrease in the amount of protein produced, particularly for Ile (bulkiest amino acid tested) and Pro (bulky and

high level of conformational constraint). The small amounts of protein produced for these mutants were likely due to degradation in the bacteria rather than accumulation in inclusion bodies, which suggests that the G129T, G129V, G129I, and G129P mutants were probably unstable and misfolded. Indeed, conformationally unstable proteins produced in *E.coli* that do not adopt a native conformation after multiple cycles of interaction with folding modulators are known to be readily degraded [17]. These data were consistent with the FOLD-X folding free energy ($\Delta G_{folding}$) calculations (Table 1), which indicated that the replacement of Gly129 by an amino acid larger than Ser greatly increases $\Delta G_{folding}$. Knowing that the $\Delta G_{folding}$ of the native state of a protein and the $\Delta G_{folding}$ of its unfolded state may differ by only 5 kcal/mol [18], the small amounts of G129T, G129V, G219I, and G219P protein may be accounted for by protein instability, misfolding and subsequent degradation [17]. Conversely, the G129A and G129S mutants (corresponding to the most conservative replacements of Gly129) were produced in similar amounts (Fig. 2) and had a similar structure to the WT MlNAT1 enzyme as observed by intrinsic fluorescence spectroscopy (not shown). These results are consistent with the similar $\Delta G_{folding}$ values calculated for the G129A, G129S, and WT proteins ($\Delta\Delta G_{folding} \sim 1$ kcal/mol; Table 1). Nonetheless, G129S was slightly less stable than the G129A and WT MlNAT1 enzymes (Fig. 4), consistent with the slightly larger size of Ser (73 $Å^3$) than of Ala (67 $Å^3$) and Gly (48 $Å^3$). Therefore, the introduction of certain bulky residues at Gly129 location of the active-site P-loop, causes major structural changes due to steric hindrance in the active site. This conclusion is supported by the major contribution of the van der Waals terms to the increase in $\Delta G_{folding}$ of the mutants. Previous structural studies [5] have suggested that the presence of a residue with a small side chain—Gly or Ala—at this active-site position allows the adjacent active-site α-helix and the β-strand to pack closely together. If this is indeed the case, then steric hindrance at the Gly129 position would probably lead to disruption of the specific packing of active-site amino acids (including those of the active-site P-loop) and to subsequent overall protein structure alteration/misfolding. Interestingly, it has been shown that the replacement of a conserved Gly residue in one of the loops of glutathione *S*-transferase P1-1 (GSTP1-1) with bulky residues (such as Val) decreases protein stability and results in major structural changes/misfolding due to steric hindrance [19]. No significant effect on GSTP1-1 structure was observed when the Gly residue was replaced by an Ala residue [19].

The NAT activity of the mutants closely matched the data for protein production. Indeed, the mutant proteins produced in small amounts—G129T, G129V, G129I, and G129P—also had very low catalytic activities. This suggests that Gly129 substitution has an indirect effect on the catalytic properties of the enzyme, as structural studies have shown that this residue is not involved in catalysis or substrate binding [3,9,10]. In contrast, G129A and the WT enzymes were found to have similar enzymatic properties. Conversely, the catalytic efficiency of G129S was significantly lower (by a factor of up to 2.6) than that of the WT MlNAT1 and G219A mutant. The lower catalytic efficiency of the G129S mutant resulted mainly from changes in the binding properties of this enzyme with a Km_{app} 2 times lower with respect to the WT MlNAT1 and G129A mutant. As the active-site P-loop is involved in substrate binding, our data suggest that the changes in the catalytic properties of the Gly129 mutants may result, at least partly, from changes in the conformational properties of the active-site P-loop due to steric hindrance at the Gly129 position. More importantly, our results demonstrate that this Gly129 position is important not only for maintaining the active site in a suitable conformation, but also for maintaining the overall structural integrity of the MlNAT1 enzyme.

Acknowledgments

This work was supported by ARC (*Association pour la Recherche sur le Cancer*), AFM (*Association Française contre les Myopathies*) and DGA (*Délégation Générale de l'Armement*). We also acknowledge support from Agence Française de Sécurité Sanitaire de l'Environnement et du Travail (AFSSET).

References

[1] B. Riddle, W.P. Jencks, Acetyl-coenzyme A: arylamine *N*-acetyltransferase. Role of the acetyl-enzyme intermediate and the effects of substituents on the rate, J. Biol. Chem. 246 (1971) 3250–3258.
[2] J.M. Dupret, F. Rodrigues-Lima, Structure and regulation of the drug-metabolizing enzymes arylamine *N*-acetyltransferases, Curr. Med. Chem. 12 (2005) 311–318.
[3] J. Sandy, A. Mushtaq, S.J. Holton, P. Schartau, M.E. Noble, E. Sim, Investigation of the catalytic triad of arylamine *N*-acetyltransferases: essential residues required for acetyl transfer to arylamines, Biochem. J. 390 (2005) 115–123.
[4] G.H. Goodfellow, J.M. Dupret, D.M. Grant, Identification of amino acids imparting acceptor substrate selectivity to human arylamine acetyltransferases NAT1 and NAT2, Biochem. J. 348 (Pt 1) (2000) 159–166.
[5] F. Rodrigues-Lima, C. Deloménie, G.H. Goodfellow, D.M. Grant, J.M. Dupret, Homology modelling and structural analysis of human arylamine *N*-acetyltransferase NAT1: evidence for the conservation of a cysteine protease catalytic domain and an active-site loop, Biochem. J. 356 (2001) 327–334.
[6] I.M. Westwood, S.J. Holton, F. Rodrigues-Lima, J.-M. Dupret, S. Bhakta, M.E.M. Noble, E. Sim, Expression, purification, characterisation and structure of *Pseudomonas aeruginosa* arylamine *N*-acetyltransferase, Biochem. J. 385 (2005) 605–612.
[7] S.J. Holton, J. Dairou, J. Sandy, F. Rodrigues-Lima, J.M. Dupret, M.E.M. Noble, E. Sim, Structure of *Mesorhizobium loti* arylamine *N*-acetyltransferase 1, Acta Cryst. F61 (2005) 14–16.
[8] S. Boukouvala, G. Fakis, Arylamine *N*-acetyltransferases: what we learn from genes and genomes, Drug Metab. Rev. 37 (2005) 511–564.
[9] J. Sandy, S. Holton, E. Fullam, E. Sim, M. Noble, Binding of the antitubercular drug isoniazid to the arylamine *N*-acetyltransferase protein from *Mycobacterium smegmatis*, Protein Sci. 14 (2005) 775–782.
[10] N. Zhang, L. Liu, F. Liu, C.R. Wagner, P.E. Hanna, K.J. Walters, NMR-based model reveals the structural determinants of mammalian

arylamine *N*-acetyltransferase substrate specificity, J. Mol. Biol. 363 (2006) 188–200.

[11] F. Rodrigues-Lima, J. Dairou, C.L. Diaz, M.C. Rubio, E. Sim, H.P. Spaink, J.M. Dupret, Cloning, functional expression and characterization of *Mesorhizobium loti* arylamine *N*-acetyltransferases: rhizobial symbiosis supplies leguminous plants with the xenobiotic *N*-acetylation pathway, Mol. Microbiol. 60 (2006) 505–512.

[12] E.W. Brooke, S.G. Davies, A.W. Mulvaney, F. Pompeo, E. Sim, R.J. Vickers, An approach to identifying novel substrates of bacterial arylamine *N*-acetyltransferases, Bioorg. Med. Chem. 11 (2003) 1227–1234.

[13] A. Cornish-Bowden (Ed.), Fundamentals of Enzyme Kinetics, Portland press, Berlin, 2001.

[14] R. Guerois, J.E. Nielsen, L. Serrano, Predicting changes in the stability of proteins and protein complexes: a study of more than 1000 mutations, J. Mol. Biol. 320 (2002) 369–387.

[15] A.J. Fretland, M.A. Leff, M.A. Doll, D.W. Hein, Functional characterization of human *N*-acetyltransferase 2 (NAT2) single nucleotide polymorphisms, Pharmacogenetics 11 (2001) 207–215.

[16] J. Dairou, D. Flatters, A.F. Chaffotte, B. Pluvinage, E. Sim, J.M. Dupret, F. Rodrigues-Lima, Insight into the structure of *Mesorhizobium loti* arylamine *N*-acetyltransferase 2 (MLNAT2): a biochemical and computational study, FEBS Lett. 580 (2006) 1780–1788.

[17] F. Baneyx, M. Mujacic, Recombinant protein folding and misfolding in *Escherichia coli*, Nat. Biotechnol. 22 (2004) 1399–1408.

[18] A. Fersht, Structure and mechanism in protein science. A guide to enzyme catalysis and protein folding, first ed., New York, 1999.

[19] G.K. Kong, G. Polekhina, W.J. McKinstry, M.W. Parker, B. Dragani, A. Aceto, D. Paludi, D.R. Principe, B. Mannervik, G. Stenberg, Contribution of glycine 146 to a conserved folding module affecting stability and refolding of human glutathione transferase p1-1, J. Biol. Chem. 278 (2003) 1291–1302.